Research Paper

Genomic deletion of TLR2 induces aggravated white matter damage and deteriorated neurobehavioral functions in mouse models of Alzheimer's disease

Chao Zhou[1,2,*], Xiaoyu Sun[1,2,*], Yuting Hu[1,2,*], Jiaxing Song[1,2], Shuyu Dong[1,2,3], Delian Kong[1,2], Yuqiao Wang[1,2], Xiaodong Hua[4,5], Jingjing Han[1,2], Yan Zhou[1,2], Guoliang Jin[1,2], Xinxin Yang[1,2], Hongjuan Shi[1,2], Zuohui Zhang[1,2], Fang Hua[1,2]

[1]Department of Neurology, The Affiliated Hospital of Xuzhou Medical University, Xuzhou, China
[2]Institute of Neurological Diseases, Xuzhou Medical University, Xuzhou, China
[3]Department of Neurology, Xuzhou Central Hospital, Xuzhou, China
[4]Augusta University/University of Georgia Medical Partnership, Athens, GA 30606, USA
[5]Medical College of Georgia, Augusta University, Augusta, GA 30606, USA
*Equal contribution

Correspondence to: Fang Hua; **email:** huafang@xzhmu.edu.cn
Keywords: TLR2, Alzheimer's disease, MRI, white matter damage, neurobehavioral function
Received: February 25, 2019 **Accepted:** September 2, 2019 **Published:** September 11, 2019

Copyright: Zhou et al. This is an open-access article distributed under the terms of the Creative Commons Attribution License (CC BY 3.0), which permits unrestricted use, distribution, and reproduction in any medium, provided the original author and source are credited.

ABSTRACT

Toll-like receptor-2 (TLR2), a member of the TLR family, plays an important role in the initiation and regulation of immune/inflammation response, which is a critical mechanism underlying Alzheimer's disease (AD). To clarify the role of TLR2 in the pathological process of AD, in the present study, TLR2 knockout plus APPswe/PSEN1dE9 transgenic mice (AD-TLR2KO) were generated. Neurobehavioral tests and brain MRI scan were conducted on mice at the age of 12 months. Additionally, neuron loss was evaluated using NeuN staining. Amyloid β protein (Aβ), glial fibrillary acidic protein (GFAP), endogenous ligands for TLR2, and the activation of downstream signaling of TLR2 in mouse brains were detected by immunohistochemistry and Western blots. The results demonstrated that TLR2 deficit induced learning disabilities, decreased spontaneous activity, increased anxiety and depression, and led to white matter damage (WMD), brain atrophy, loss of neurons, and glial activation. Moreover, TLR2 deficit aggravated impaired neurobehavioral functions and WMD in AD mice, but did not affect the Aβ deposition in mouse brains. Our data indicate that the genomic deletion of TLR2 impairs neurobehavioral functions, induces WMD and brain atrophy, and increases the activation of astrocytes, which in turn aggravate the symptoms of AD through a non-Aβ mechanism.

INTRODUCTION

Alzheimer's disease (AD) is a neurodegenerative disease typified by chronic inflammation and neuronal loss in the brain [1, 2]. In patients with familial Alzheimer's disease (FAD), mutations in the APP gene, PSEN1 gene, and PSEN2 gene were found. In addition, other candidate genes associated with AD were also identified, of which the polymorphic apolipoprotein E (apoE) gene was reported to be the most related [3]. Due to these genetic mutations, the deposition of Aβ and the hyperphosphorylation of the tau-protein appear in the brain [4, 5], inducing the loss of neurons, the activation of astrocytes, and the hyperactivation of microglia cells [6, 7]. Activated microglia and astrocytes release pro-inflammatory cytokines, leading to inflammatory responses, which are involved in not only neuronal death and neurofibrillary tangle formation but also in

Aβ clearance and neuroregeneration [8]. Substantial evidence has demonstrated that inflammation plays a key role in the pathological processes of AD [9]. Excessive inflammation associated with the deposition of Aβ and the hyperphosphorylation of the tau-protein results in neuronal loss and white matter damage (WMD) [10–12]. On the other hand, moderate inflammation is helpful for eliminating the deposition of Aβ and for neuroregeneration [13]. The mechanisms underlying the regulation and modulation of inflammation in AD brains are, however, unclear at present.

Toll-like receptors (TLRs) are a family of type-1 transmembrane receptors. TLRs, possessing the toll/interleukin-1 receptor (TIR) domain and leucine-rich repeat (LRR) motifs, regulate host defensive response via the myeloid differentiation primary response 88 (MyD88)-dependent pathway and/or the MyD88-independent signaling pathway [14]. Activated by ligands, TLRs recruit serial downstream kinases, leading to the activation of nuclear factor kappa B (NF-kB) and/or interferon regulatory factor 3 (IRF3) and resulting in the release of pro-inflammatory factors and anti-inflammatory factors [15]. TLRs were found to be expressed in neural precursor cells, neurons, and glial cells, and are involved in the immune functional maturation of microglia, as well as in the differentiation and development of neurons [16].

Recently, the role of TLRs in the AD pathological process has attracted the attention of investigators. Previous studies demonstrated that modulating TLRs results in changes in pathology and neurobehavioral functions in AD rodent models [17–20]. For example, a deficiency of TLR4 in AD models up-regulated cytokines and glial cell activation [21]. The activation of TLR4 by agonists improved cognitive impairments in rat models of AD [22]. TLR2, a member of the TLR family but different from TLR4 and other TLRs, is mediated through MyD88 alone. Recent studies demonstrated that activated bone-marrow-derived microglia (BMDM) could uptake Aβ and help to clear Aβ deposition [23], while TLR2 deficit BMDM could not perform its Aβ clearance function; moreover, TLR2 deficiency aggregated cognitive dysfunction in APP/PS1 transgenic mice [24, 25]. In contrast, other studies have reported that long-term administration of the TLR2 inhibitor in AD mice could reduce Aβ aggregation and glial activation [26], and that TLR2 gene knockout and the blocking of the interaction between TLR2 and MyD88 could attenuate the neurotoxicity and pathological changes of AD [27, 28]. While these contradictory phenomena could be interpreted as the consequence of different experimental conditions, such as differences in animal models, observed time points, and cell types, it is nonetheless apparent that TLR2 does play a role in the process of AD, although the exact effect remains to be elucidated.

To clarify the role of TLR2 in the pathological process of AD, in the present study, TLR2 knockout (KO) plus APPswe/PSEN1dE9 transgenic mice (AD-TLR2KO) were generated. Cognitive and emotional behavioral tests were conducted on the mice at the age of 12 months. Cortical thickness and white matter integrity were evaluated using brain magnetic resonance imaging (MRI). Neuron loss was evaluated using NeuN staining. Aβ, GFAP, proteins related to synaptic function, endogenous ligands for TLR2, and the activation of downstream signaling of TLR2 in brain tissue were detected by Western blots and immunohistochemistry (IHC) staining.

RESULTS

Genomic deletion of TLR2 induced cognitive impairment

Learning and memory function were detected at the age of 12 months. As shown in Figure 1A and 1B, the latencies (the time taken to find the hidden platform during the acquisition/learning phase) in AD mice were significantly longer than those in wild type (WT) control mice ($p<0.05$) from the 3rd day to the 7th day in the acquisition/learning phase. The latencies in TLR2KO mice were also significantly longer than those in WT control mice ($p<0.05$). Importantly, the latencies in AD-TLR2KO mice were significantly prolonged compared with those in AD mice ($p<0.05$) during the acquisition/learning phase.

Since mice have the habit of swimming along the pool, most searched the platform using an edge-type strategy on the first day of testing. As the tests progressed, WT mice converted to the tendency-type and straight-type searching strategies. Compared with WT mice, AD mice demonstrated a significantly higher ratio of the edge-type searching strategy ($p<0.05$, Figure 1C). In addition, the ratio of the edge-type strategy in TLR2KO mice was significantly higher than that in WT mice ($p<0.05$, Figure 1C). Importantly, the ratio of the edge-type strategy increased in AD-TLR2KO mice compared with AD mice ($p<0.05$, Figure 1C).

In the probe test on the 8th day, the mice were placed into water from the 3rd quadrant, which was farthest from the platform (Figure 1A). The results showed that the frequencies of crossing the platform area in AD, AD-TLR2KO, and TLR2KO mice were significantly lower than those in WT mice ($p<0.05$, Figure 1D). In addition, the time spent in the target quadrant among AD, AD-TLR2KO, and TLR2KO mice was significantly less than

that among WT mice ($p<0.05$, Figure 1E). There was no difference, however, in the frequencies of crossing the platform area or in the time spent in the target quadrant between AD and AD-TLR2KO mice.

The results indicated that TLR2 gene knockout significantly impaired learning ability and reference memory function. Moreover, TLR2 deficiency exacerbated learning impairment, but not reference memory function, in AD mice at the age of 12 months.

Genomic deletion of TLR2 decreased spontaneous activity and increased anxiety and depression

In the open field test (Figure 2A), our data indicated that, compared with WT mice, the AD, TLR2, and

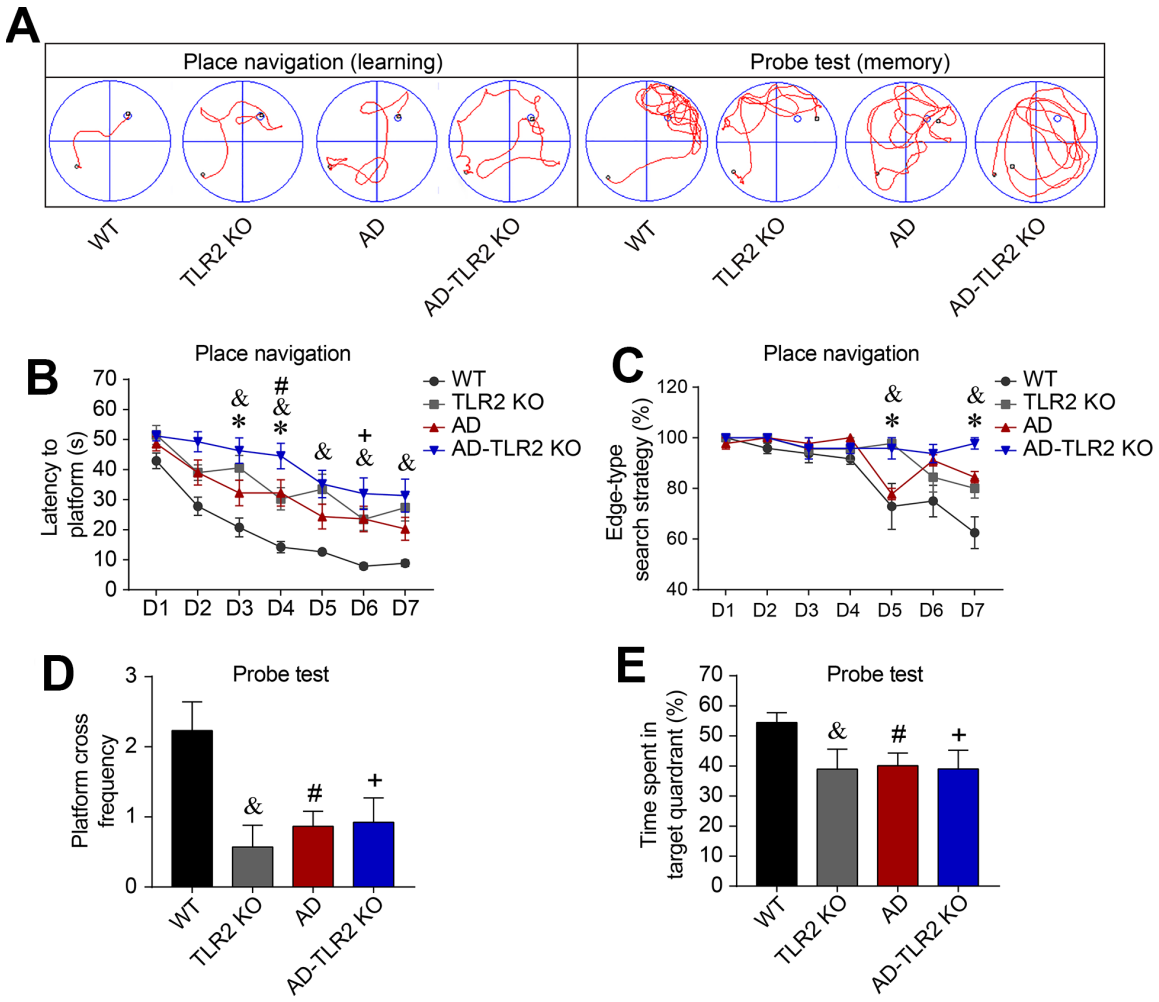

Figure 1. Genomic deletion of TLR2 accelerated cognitive impairments in mouse models of AD. Morris water maze tests (MWM) were performed on mice for seven consecutive days of place navigation processes, and a probe test was conducted on the 8th day for mice aged 12 months. (**A**) Representative track plots of MWM for place navigation and probe tests. (**B**) The latency (time to find the hidden platform) increased in TLR2 knockout mice (&: TLR2KO vs. WT, $p<0.05$), AD mice (#: AD vs. WT, $p<0.05$), and AD-TLR2KO mice (+: AD-TLR2KO vs. WT, $p<0.05$). Moreover, the latency was prolonged in AD-TLR2KO mice compared with AD mice (*: AD-TLR2KO vs. AD, $p<0.05$). (**C**) Since mice have the habit of swimming along the pool, most of the mice searched the platform using an edge-type strategy on the first day of the test. As the tests progressed, WT mice converted to the tendency-type and straight-type searching strategies. However, compared with WT mice, AD mice exhibited a significantly higher ratio of the edge-type searching strategy (#: AD vs. WT, $p<0.05$). In addition, the ratio of the edge-type strategy in TLR2KO mice was significantly higher than that in WT mice (&: TLR2KO vs. WT, $p<0.05$). Importantly, the ratio of the edge-type strategy increased in AD-TLR2KO mice compared with AD mice (*: AD-TLR2KO vs. AD, $p<0.05$). (**D** and **E**) In the probe test, the frequencies of crossing the platform area in AD, AD-TLR2KO, and TLR2KO mice were significantly lower than those in WT mice ($p<0.05$, **D**). The time spent in the target quadrant among AD, AD-TLR2KO, and TLR2KO mice was significantly less than that among WT mice ($p<0.05$, **E**). However, there was no difference in the frequencies of crossing the platform area or in the time spent in the target quadrant between AD and AD-TLR2KO mice (Note: &: TLR2KO vs. WT, $p<0.05$; #: AD vs. WT, $p<0.05$; +: AD-TLR2KO vs. WT, $p<0.05$; *: AD-TLR2KO vs. AD, $p<0.05$. n=11~15/group).

AD-TLR2KO mice exhibited significantly shorter exploration times in the central area ($p<0.05$). The exploration time among AD-TLR2KO mice was shorter than that among AD mice ($p<0.05$, Figure 2B). In addition, the total traveled distance was shorter among AD-TLR2KO mice compared with WT mice ($p<0.05$, Figure 2C). Moreover, in the tail suspension test, the rest time among AD-TLR2KO mice significantly increased compared with that among WT mice ($p<0.01$, Figure 2D). The time in the enclosed arms did not show a significant difference among the groups in the elevated plus maze test (Figure 2E).

Genomic deletion of TLR2 did not affect Aβ deposition in AD mice

The results from Western blots and immunofluorescence staining, as shown in Figure 3, demonstrated abundant Aβ deposition in the cortex and hippocampus in AD and AD-TLR2KO mice brains. The levels of Aβ were significantly higher in AD and AD-TLR2KO mice compared with those in WT and TLR2KO mice, respectively ($p<0.05$). However, there was no difference in Aβ levels between AD and AD-TLR2KO mice.

Genomic deletion of TLR2 accelerated white matter damage in AD mice

By using a 7 Tesla MRI system, the WMD in mice brains was evaluated at the age of 12 months. After MRI scanning, diffusion tensor imaging (DTI) maps were obtained (Figure 4A). Fractional anisotropy (FA), axial diffusivity (Da), mean diffusivity (MD), and radial diffusivity (Dr) values were analyzed, and quantitative analysis of the same region of interest (ROI) for each mouse was performed using DSI studio software. As shown in Figure 4A, the FA value in the external capsule (EC) area, indicating the integrity of white matter, declined in AD and AD-TLR2KO mice compared with WT and TLR2KO mice ($p<0.05$, Figure 4B). The values of Da and Dr were also associated with myelin and axonal damage. The data showed that the Da value

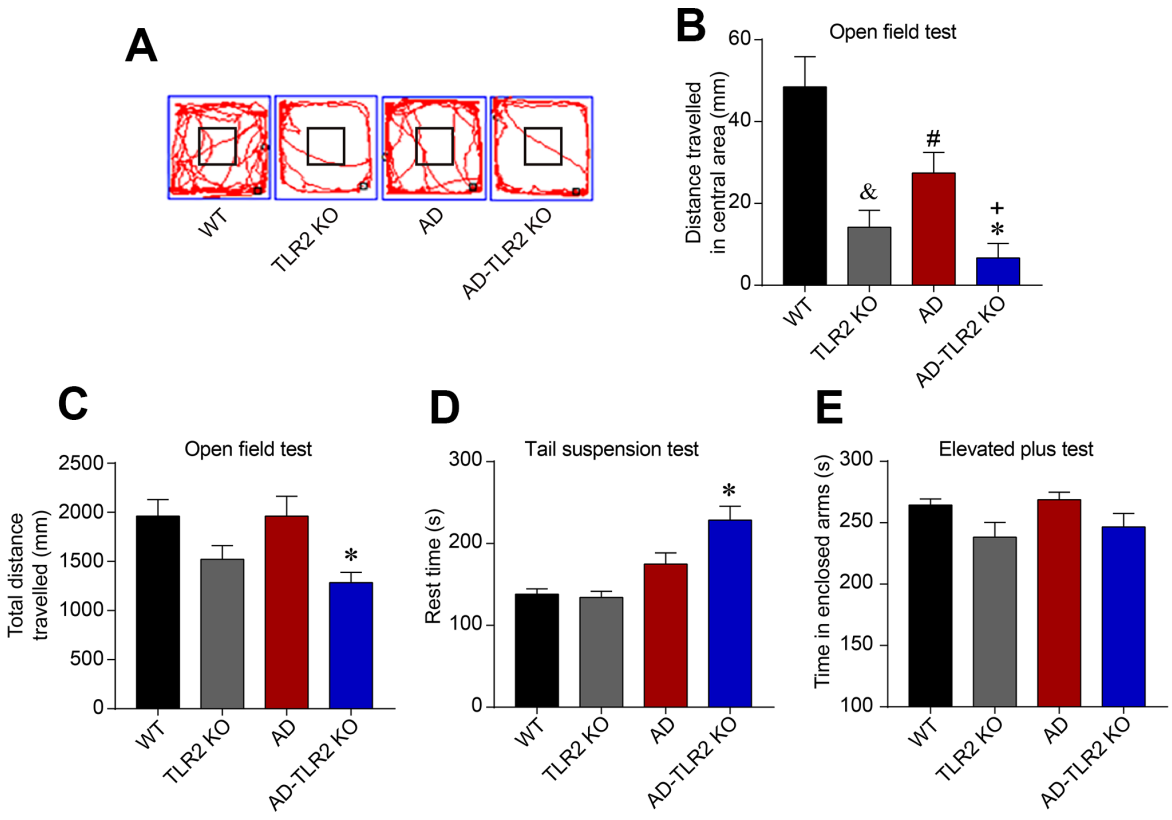

Figure 2. TLR2 knockout increased the anxiety and depression states in mouse models of AD. (**A**) Representative track plots from open field maze test. (**B**) The exploration times in the central area were significantly shorter in AD, TLR2, and AD-TLR2KO mice compared with WT mice ($p<0.05$). Moreover, the exploration time in the central area among AD-TLR2KO mice was shorter than that among AD mice ($p<0.05$). (**C**) The total traveled distance of AD-TLR2KO mice was shorter compared with WT mice ($p<0.05$). (**D**) In the tail suspension test, the rest time for AD-TLR2KO mice significantly increased compared with WT mice ($p<0.05$). (**E**) However, the time in enclosed arms did not show a significant difference among the groups in the elevated plus maze test (n=11~15/group).

decreased and the Dr value increased in AD-TLR2KO mice compared with WT mice ($p<0.05$, Figure 4C, 4D). In addition, cortical thickness was measured by Image J software on T2-weighted images obtained from Paravision software (Figure 5A). The results demonstrated that the thickness of the cortex was significantly reduced in TLR2KO mice ($p<0.05$, Figure 5B) compared with WT mice.

Genomic deletion of TLR2 increased glial activation in mouse models of AD

Glial fibrillary acidic protein (GFAP), a specific marker for astrocytes, was detected using Western blots and immunofluorescence staining. As shown in Figure 6, the level of GFAP significantly increased in AD mice and AD-TLR2KO mice compared with WT mice ($p<0.05$). Moreover, the GFAP level was higher in AD-TLR2KO mice than in AD mice ($p<0.05$).

Genomic deletion of TLR2 did not significantly affect the proteins associated with synaptic plasticity

Previous research has reported that the synaptic plasticity in AD model was damaged, which might be one explanation for the acceleration of memory deficits and disease processes. In the present study, the protein levels of synaptophysin (Syn) and postsynaptic density protein 95 (PSD95) were detected using Western blot (Figure 7). The results showed no significant differences in Syn and PSD95 protein levels among each group of 12-month-old mice.

Genomic deletion of TLR2 induced neuron loss in mouse brains

The neuronal number was evaluated at the age of 12 months by IHC staining for NeuN, a marker for neurons. As shown in Figure 8, neuronal numbers in TLR2KO

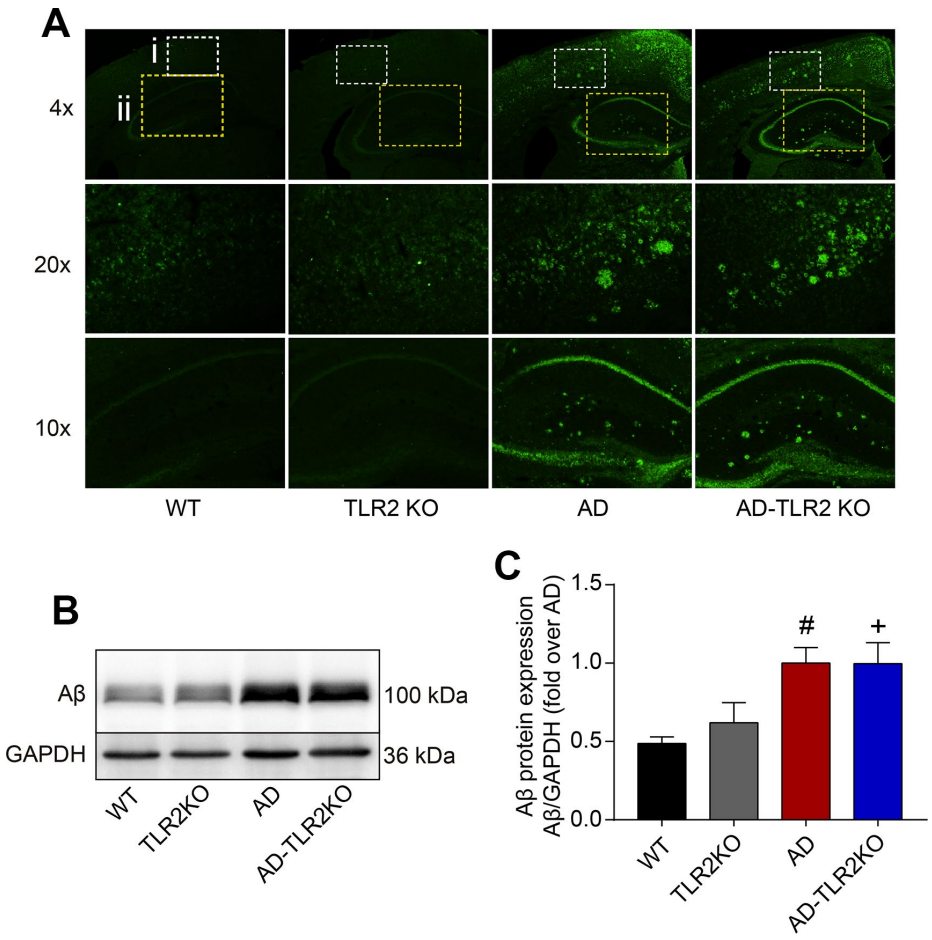

Figure 3. Aβ deposition in mouse brains. (**A**) Representative immunofluorescence images of Aβ deposition in mouse brains (4x, 20x: cortex; 10x: hippocampus). (**B**) Representative Aβ levels in brain tissues detected by Western blots. (**C**) Results from quantitative analyses of Western blots showed that Aβ levels were significantly higher in AD and AD-TLR2KO mice compared with WT and TLR2KO mice, respectively (#: AD vs. WT, $p<0.05$; +: AD-TLR2KO vs. WT, $p<0.05$). However, there was no significant difference in Aβ levels between AD and AD-TLR2KO mice (n=6 / group).

mice significantly decreased compared with those in WT mice ($p<0.05$). In addition, neuronal numbers were also lower in AD mice and AD-TLR2KO mice compared with those in WT mice ($p<0.05$). However, no significant difference in neuronal number was observed among AD, TLR2KO, and AD-TLR2KO mice ($p>0.05$).

Genomic deletion of TLR2 increased the protein level of biglycan, but not HMGB1, in AD mice

Biglycan and high mobility group box 1 (HMGB1), endogenous ligands for TLR2, were detected using Western blot. As shown in Figure 9, the protein level of

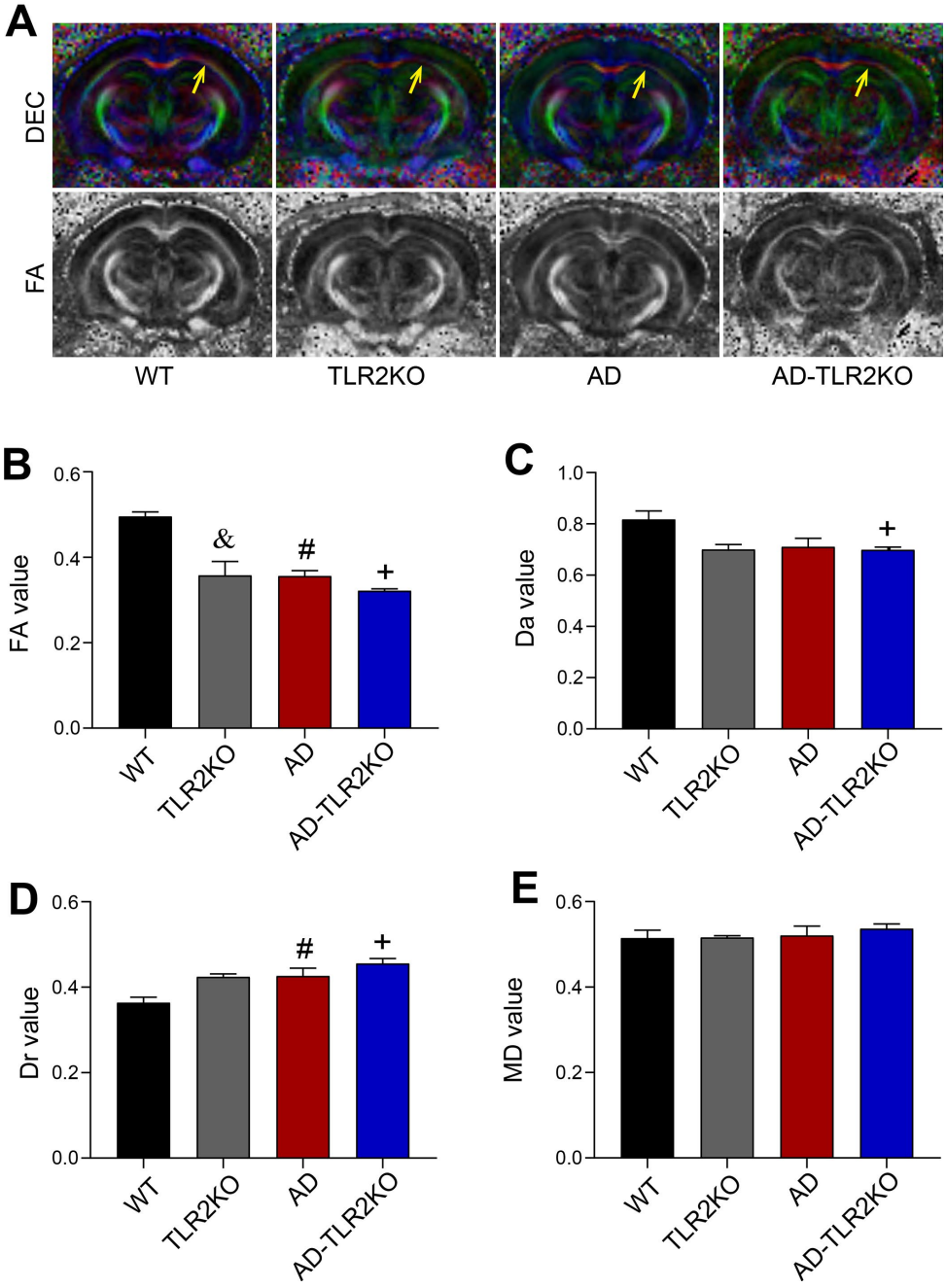

Figure 4. White matter integrity evaluated by DTI images detected by 7 Tesla MRI system. (**A**) Representative diffusion-encoded-color (DEC) map and fractional anisotropy (FA) map showing white matter injury (yellow arrow). (**B**) Quantitative analysis showed that the FA value significantly decreased in TLR2KO mice (&), AD mice (#), and AD-TLR2KO mice (+) compared with WT mice ($p<0.05$, **B**). (**C**) Axial diffusivity (Da) value decreased in AD-TLR2KO mice compared with WT mice (+: $p<0.05$). (**D**) Radial diffusivity (Dr) value increased in AD (#) and AD-TLR2KO (+) mice compared with WT mice ($p<0.05$). (**E**) There was no significant deference in the mean diffusivity (MD) value among the groups. (n= 4~6 / group).

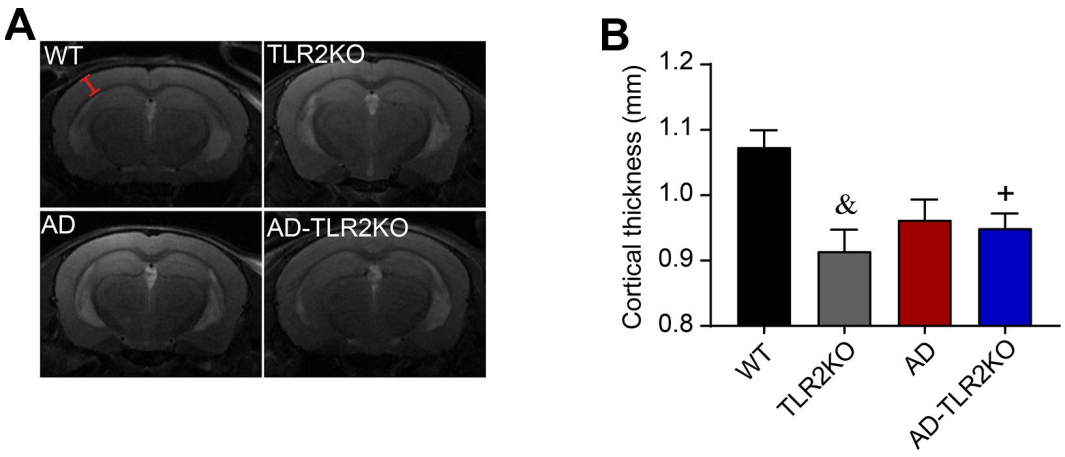

Figure 5. Thickness of cortex evaluated by T2-weighted images detected by 7 Tesla MRI system. The cortical thickness was measured by Image J software on T2-weighted images obtained from Paravision software. (**A**) Representative T2-weighted images used for measurement of cortical thickness (red line segment indicates the measured regions). (**B**) Results showed that cortical thickness was reduced in TLR2KO mice and AD-TLR2KO mice compared with WT mice (&: TLR2KO vs. WT, p<0.05; +: AD-TLR2KO vs. WT, p<0.05). (n= 4~6 / group).

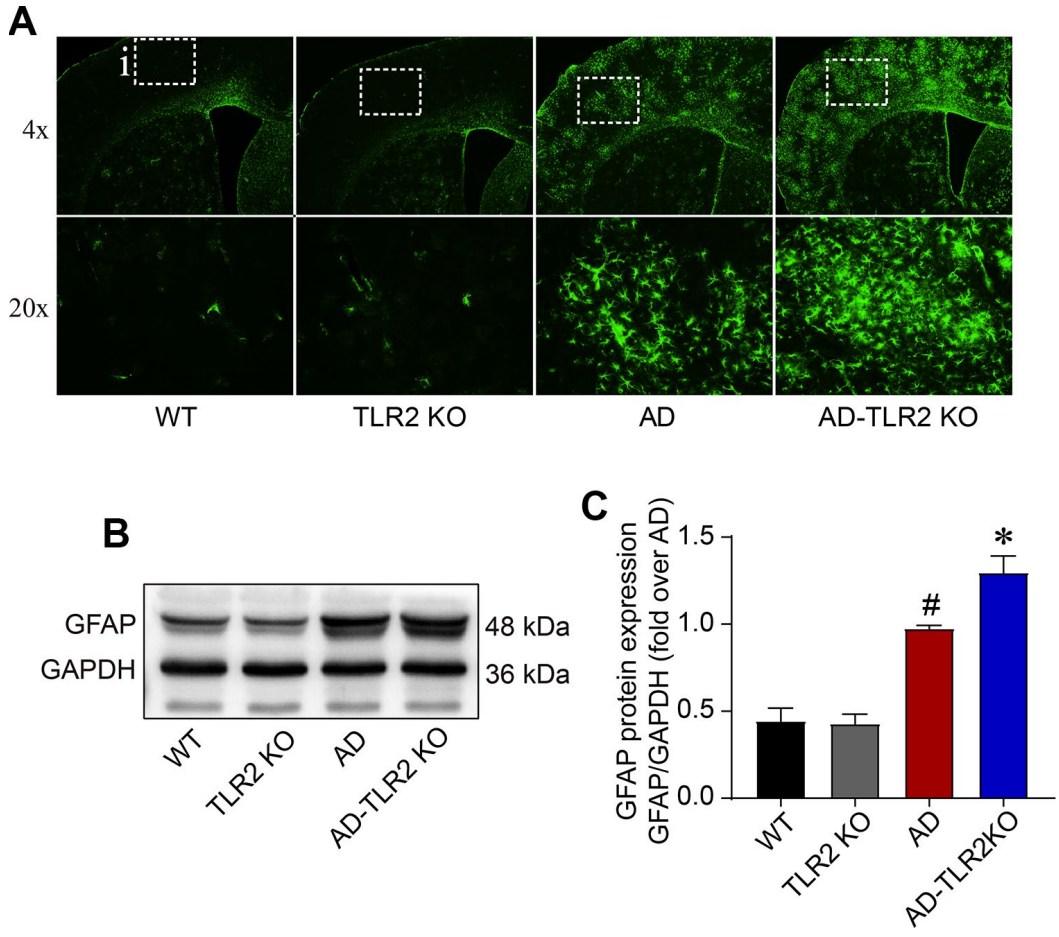

Figure 6. Levels of GFAP in mouse brains. (**A**) Representative immunofluorescence staining of GFAP, a marker of astrocytes. (**B**) Representative bands of GFAP in brain tissues detected by Western blots. (**C**) GFAP significantly increased in AD mice and AD-TLR2KO mice compared with WT and TLR2 mice, respectively (#: AD vs. WT, p<0.05; +: AD-TLR2KO vs. WT, p<0.05). Moreover, the level of GFAP in AD-TLR2KO mice was significantly higher than that in AD mice (*: AD-TLR2KO vs. AD, p<0.05). (n= 6 / group).

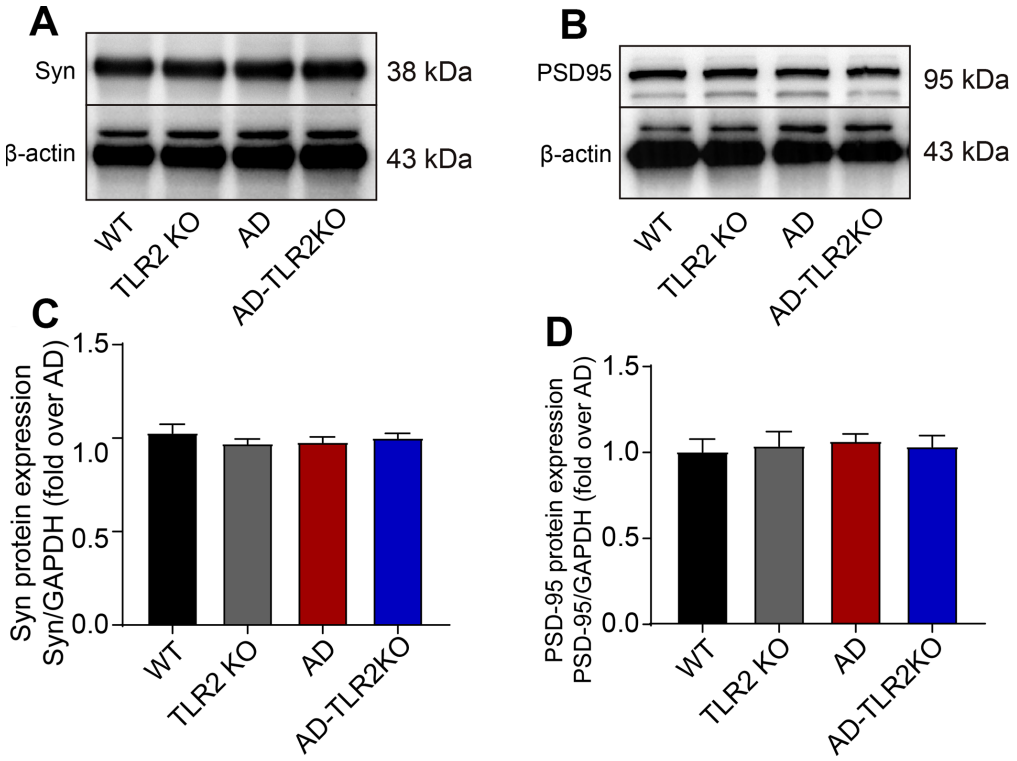

Figure 7. Levels of synaptophysin (Syn) and PSD95 in mouse brains. (**A**) Representative image of Western blots for Syn. (**B**) Representative image of Western blots for PSD95. (**C**, **D**) There was no significant difference in the levels of Syn (**C**) and PSD95 (**D**) between AD and AD-TLR2KO mice. (n= 6 / group).

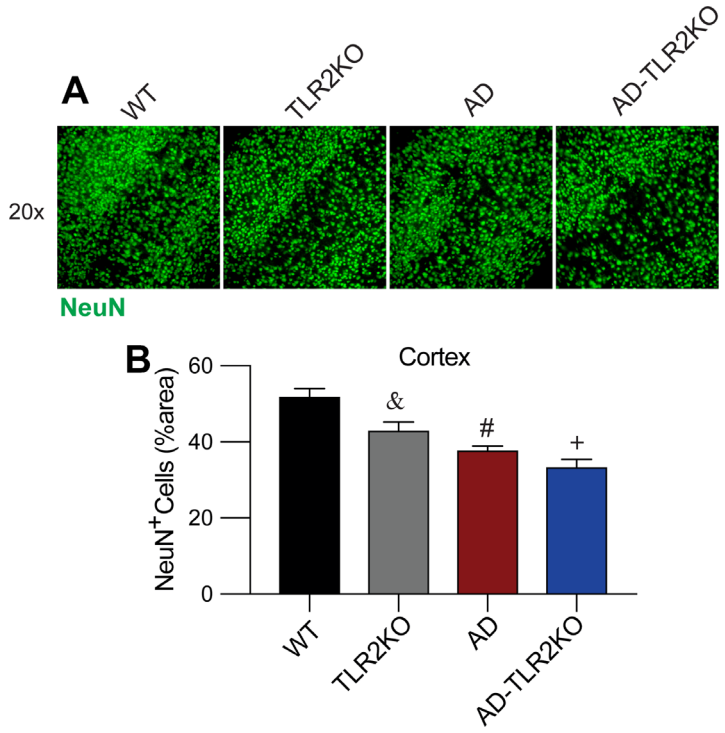

Figure 8. TLR2 deficiency resulted in neuronal loss in mouse brains. (**A**, **B**) Neuronal density detection and quantification analysis indicated a lower capacity of NeuN⁺ cells in AD, TLR2KO, and AD-TLR2KO mice when compared with WT mice (n=6 for each group, $p<0.05$).

biglycan in AD-TLR2KO mice was significant higher that that in WT, TLRKO, and AD mice ($p<0.05$). However, there was no significant difference in HMGB1 among the four groups at the age of 12 months ($p>0.05$).

Genomic deletion of TLR2 decreased the activation of TLR-MyD88-NFκB signaling in AD mose brains

MyD88 is a key adaptor protein in TLR-mediated signaling pathways. Activation of TLR2 mediates MyD88 alone, leading to the phosphorylation of NFκB and the regulation of inflammatory responses. As shown in Figure 10, MyD88 and p-NFκB significantly increased in the brains of AD mice ($p<0.05$), but were inhibited in AD-TLR2KO mice ($p<0.05$).

DISCUSSION

Prior research has shown that AD is a heterogeneous disease involving multiple pathogenic factors, including β-amyloid deposition, tau-protein hyperphosphorylation, and inflammatory reaction, among other mechanisms [29], of which immune inflammatory response is the core pathological mechanism. The imbalance of immune inflammatory response and its regulatory mechanism promotes the occurrence and development of AD. Many immune inflammatory factors are involved in AD [30], including microglia, peripheral immune cells, the interleukin family, the tumor necrosis factor family, and TLR-mediated transduction pathways [7, 8, 13, 31, 32].

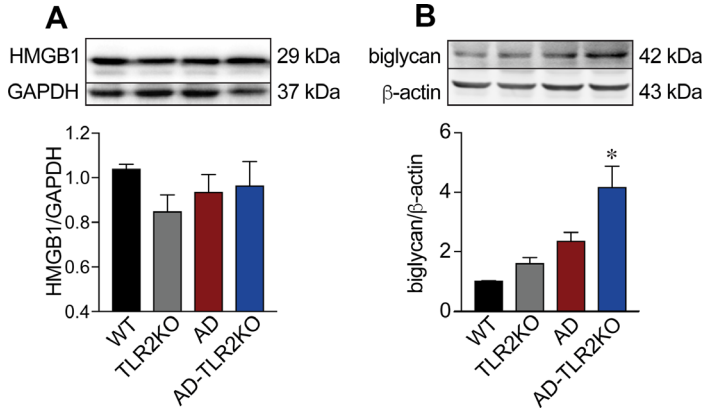

Figure 9. Expression of endogenous ligands for TLR2. (**A**) Expression of biglycan in AD-TLR2KO mice increased significantly compared with that in WT, AD, and TLR2KO mice ($p<0.05$). (**B**) HMGB1 in the four groups did not show a significant difference ($p>0.05$).

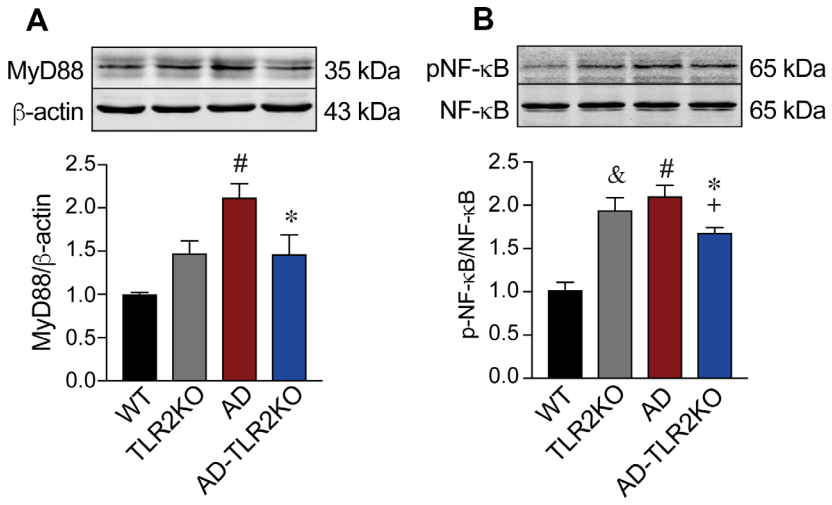

Figure 10. Activation of MyD88-NFκB signaling. Expression of MyD88 significantly increased in AD mice compared with WT mice ($p<0.05$). The increased MyD88 was inhibited in AD-TLR2KO mice compared with AD mice ($p<0.05$). Expression of pNF-kB significantly increased in AD mice compared with WT mice ($p<0.05$). The phosphorylation of NF-kB was inhibited in AD-TLR2KO mice compared with AD mice ($p<0.05$).

TLRs are a type I transmembrane receptor superfamily that plays an important role in the induction and regulation of immune inflammatory responses. At present, at least 13 TLRs have been found in mammals, including 10 TLRs (TLR1 to TLR10) in humans and 12 in mice (TLR1 to TLR9, TLR11 to TLR13) [33]. Activated by their ligands, TLRs activate downstream protein kinases through regulatory proteins, leading to the activation of nuclear transcription factors (NFκB) and/or the interferon regulatory factor (IRF), as well as to the release of immune inflammatory factors [33, 34]. TLR signaling is mainly mediated by two regulatory proteins, MyD88 (myeloid differentiation factor 88) and TRIF (TIR-domain-containing adapter-inducing interferon-β), which are, respectively, mediators of the MyD88-dependent signaling pathway and the TRIF-dependent (MyD88-independent) signaling pathway.

Recently, the role and mechanism of TLRs in the development of AD, and the role of specific drugs for TLRs in AD, have been reported [35]. TLR2, TLR4, TLR5, TLR7, and TLR9 mRNAs were found to be significantly up-regulated in the plaque-associated brain tissue of aged APP23 transgenic mice compared to the plaque-free tissue [36]. Expressions of mRNAs and proteins of TLR2 and TLR4 in peripheral blood mononuclear cells (PBMCs) were markedly elevated in late-onset AD (LOAD) patients [37]. Levels of TLR4-dependent cytokines, such as tumor necrosis factor (TNF)-alpha, interleukin (IL)-1beta, IL-10, and IL-17, in the brains of transgenic AD mice were significantly higher than those in non-transgenic WT mice [38]. Behavioral, molecular, and electrophysiological evidence indicates that early minor stimulation of microglial TLR2 and TLR4 receptors attenuates AD-related cognitive deficits in rats [39]. These data strongly suggest that TLR signaling is involved in AD progression and can be a new therapeutic target for AD.

TLR2, different from other TLRs, is only propagated through the MyD88-dependent pathway. Previous studies have indicated that mice lacking TLR2 receptors are largely protected against ethanol-induced cytokine and chemokine release, as well as against behavioral-associated effects during alcohol abstinence [40]. Activation of TLR2 by intracerebroventricular injection of its ligand, Pam3CSK4, induced sickness behavior symptoms, including anorexia, hypoactivity, and hyperthermia [41]. Recent studies on the role of TLR2 in AD have yielded conflicting results. For example, one study revealed that inhibiting TLR2 by the anti-TLR2 antibody improved performance in spatial learning by decreasing microglial and astroglial activation, and by reducing Aβ plaque burden [26]. However, another study reported that the intracerebroventricular administration of low-dose TLR2 ligands reduced disturbances in spatial and working memory and reversed the impaired long-term potentiation induced by Aβ [39].

To further clarify the effect of TLR2 on neurobehavioral and pathological changes in AD, in the present study, we used APPswe/PSEN1dE9 transgenic (AD, $App^{+}Psen1^{+}$) mice and TLR2 gene knockout (TLR2KO, $Tlr2^{-/-}$) mice to generate $Tlr2^{-/-}App^{+}Psen1^{+}$ (AD-TLR2KO) mice. Neurobehavior functions in the mice were evaluated with different gene types at the age of 12 months. The data from the Morris water maze (MWM) demonstrated that the genomic deletion of TLR2 alone prolonged the latencies in finding the hidden platform during the acquisition/learning phase, decreased the frequencies of crossing the platform area, reduced the time spent in the target quadrant, and increased the ratio of the edge-type strategy. Moreover, the genomic deletion of TLR2 prolonged the latencies in finding the hidden platform during the acquisition/learning phase and increased the ratio of the edge-type strategy. The results indicated that the TLR2 deficit alone impaired learning ability and reference memory function, and that this deficit also exacerbated learning impairment, but not reference memory function, in AD mice at the age of 12 months. Open field tests demonstrated that TLR2KO decreased exploration times in the central area among AD mice as well as the total traveled distance. In the tail suspension test, the rest time significantly increased in AD-TLR2KO mice when compared with WT mice. These data indicate that the genomic deletion of TLR2 significantly aggravated the increased anxiety and depression in AD mice at the age of 12 months.

Diffusion tensor imaging (DTI) is a vital, non-invasive method for characterizing microstructural changes or differences with neuropathology and treatment [42, 43]. To evaluate brain damage, in the present study, diffusion tensor images were obtained and analysis of selected ROIs from ECs was performed by using a 7.0-T BioSpec 70/20 MRI scanner and diffusion spectrum magnetic resonance imaging (DSI) studio post-analysis software. The FA value represents brain white matter integrity, which is highly sensitive to microstructural changes. Da and Dr are indicators of myelination and axonal damage. The mean diffusivity (MD) value may serve as a marker of tissue water in edema and proliferation in neoplasia [42, 44, 45]. Our results demonstrated that the FA value significantly decreased in TLR2KO, AD, and AD-TLR2KO mice. In addition, the values of Da decreased, while those of Dr increased, in AD-TLR2KO mice compared with WT mice. The cortical thickness measured from T2-weighted images decreased in TLR2KO and AD-TLR2KO mice compared with WT mice. These data indicate that the TLR2 deficit was involved in WMD, myelination and axonal impairment, and brain atrophy, and further aggravated WMD in AD

mice. Impaired WMD might be a mechanism by which the TLR2 deficit induces neurobehavioral dysfunction.

Neuropathology in AD is characterized by the deposition of Aβ, senile plaques, and neurofibrillary tangles (NFTs). Gliosis and increased inflammation play important roles in the disease's pathogenesis. A previous study demonstrated that low-dose TLR2 ligands decreased Aβ deposits [39]. Conversely, other studies reported that blocking TLR2 with the anti-TLR2 antibody reduced Aβ plaque burden in APP/PS1 mice [26], and that the disruption of TLR2–MyD88 interaction inhibited hippocampal glial activation and reduced Aβ burden in 5XFAD mice [28]. To understand the mechanisms underlying the effect of the TLR2 deficit on impaired neurobehavioral functions, we detected Aβ deposition in mouse brains. Our data showed that Aβ deposition significantly increased in AD, but not in TLR2KO, mice. The increased Aβ deposition in AD mice was not inhibited in AD-TLR2KO mice. The data indicated that the TLR2 deficit resulted in the impairment of neurobehavioral functions, possibly via a non-Aβ mechanism.

Glial activation and inflammatory reaction are important self-protection mechanisms [8]. However, excessive inflammatory response is detrimental and accelerates disease process [46]. Many studies have shown excessive astrocyte gliosis and inflammation in patients with AD and in animal models of AD [31, 47]. Our data demonstrated that GFAP, a marker for astrocytes, significantly increased in AD mice compared with WT mice. Moreover, the increased GFAP was enhanced in AD-TLR2KO mice. The data indicated that the TLR2 deficit increased GFAP activation in AD mice, which might be a mechanism by which the TLR2 deficit induces the impairment of neurobehavioral functions.

Previous studies have reported that synaptic function is impaired in AD [48–50]. To investigate the effect of TLR2 on synaptic plasticity, we detected the protein levels of postsynaptic density 95 (PSD-95) and synaptophysin (Syn) in brain tissue. The results demonstrated no difference in the levels of PSD-95 and Syn among the groups, which in turn indicates that TLR2 deficiency does not lead to the changes in proteins associated with synaptic plasticity in mice at the age of 12 months.

One of the most important pathological characteristics in AD brains is the loss of neurons. In the present study, neuronal numbers were evaluated in the brains of mice at the age of 12 months by IHC staining for a neuronal marker, NeuN. The results showed (Figure 8) that neuronal numbers significantly decreased in TLR2KO, AD, and AD-TLR2KO mice compared with WT mice ($p<0.05$). However, no further decreased neuronal numbers were observed in AD-TLR2KO mice compared with AD mice ($p>0.05$). These data indicate that TLR2 deficiency was not able to induce the loss of neurons in AD brains. In contrast, TLR2 deficiency alone induced the loss of neurons in brains without AD.

The classic hallmarks of AD include the formation of Aβ plaque deposits and NFTs. However, the mechanisms underlying the initiation and progression of AD remain unclear. Recent studies have demonstrated that endogenous danger signals stimulate innate immune cells via TLR2 and TLR4 and accelerate inflammatory responses [51]. Biglycan, one prototype extracellular matrix-derived damage-associated molecular pattern, functions as an endogenous agonist of TLR2/4 and mediates sterile inflammation through TLR2- and/or TLR4-dependent signaling pathways [52]. Another central endogenous inflammatory mediator, HMGB1, when interacting with TLR signaling pathways, contributes to the pathogenesis of several inflammatory disorders [53]. However, our data failed to show increased protein levels of biglycan and HMGB1 in AD mice compared with WT mice. This phenomenon could be interpreted as meaning that since the mice used in the present study were 12 months old, some biochemical reactions occurring in the early stage of the disease are not observable in the late stage. Interestingly, TLR2 deficiency significantly increased the protein level of biglycan, but not HMGB1, indicating that TLR2 might play an important role in the clearance of biglycan.

TLR2 signaling is mediated via the MyD88-dependent pathway, leading to the phosphorylation of NFκB and to inflammatory responses. Previous studies reported that the expression of TLRs was up-regulated and TLR-mediated inflammation was activated in AD brains [36–38]. Our data, showing increased protein levels of MyD88 and p-NFκB in AD mice at the age of 12 months, indicate that the TLR downstream MyD88-dependent pathway was activated in AD brains. In addition, increased MyD88 and p-NFκB were inhibited in AD-TLR2KO mice, indicating that, in the late stage of AD, the activation of MyD88-dependent signaling is mediated through TLR2.

In summary, the present study demonstrated that the genomic deletion of TLR2 induced impaired neurobehavioral function, WMD and loss of neurons, brain atrophy, and the activation of astrocytes. TLR2 deficiency exacerbated impaired neurobehavioral function and enhanced the activation of astrocytes in AD brains without affecting Aβ deposition. Further studies on molecular mechanisms, especially in the early stage of AD, must be conducted. In addition, since TLR signaling is involved in the pathology of AD, it has been

considered as a therapeutic target for AD. Several studies have demonstrated that the activation or inhibition of TLR2 by an exogenous reagent could attenuate impaired neuronal function and pathological changes in AD models. However, the reported results have been controversial. Therefore, the exact effect of TLR2 agonists/antagonists on neurobehavioral functions and pathological changes in AD, their dose–effect relationship, and the time window for treatments require further investigation.

MATERIALS AND METHODS

Animal generation and experimental design

APPswe/PSEN1dE9 transgenic (AD, $App^{+}Psen1^{+}$) mice and TLR2 knockout (TLR2KO, $Tlr2^{-/-}$) mice were purchased from the Animal Model Research Center of Nanjing University, China. Step 1 involved breeding TLR2KO and AD mice together to generate $Tlr2^{+/-}App^{+}Psen1^{+}$ mice and $Tlr2^{+/-}$ mice. Step 2 combined $Tlr2^{+/-}App^{+}Psen1^{+}$ to generate $Tlr2^{-/-}App^{+}Psen1^{+}$ (AD-TLR2KO) mice. Meanwhile, $Tlr2^{+/-}$ mice were mated with each other to generate $Tlr2^{-/-}$ (TLR2KO) mice and $Tlr2^{+/+}$ (WT) mice. Step 3 involved breeding $App^{+}Psen1^{+}$ mice with each other to generate $App^{+}Psen1^{+}$ (AD) mice. The 3rd generation of the mice was used in our experiment. All the mice were bred at the Experimental Animal Center of Xuzhou Medical University and were kept in the same housing conditions (temperature, 22–23°C; 12h light-dark cycle; food and water were available ad libitum). All aspects of animal care and experimental protocols were approved by the Xuzhou Medical University Committee on Animal Care.

Morris water maze (MWM)

The MWM system (Zhenghua Biological Instruments, China) was used to evaluate spatial learning and reference memory according to the processes described previously in our laboratory [33]. Briefly, the inner diameter of the circular pool was set at 122cm, and the depth was set at 40cm. All sides of the pool were painted white to create a strong contrast with the mice. A circular platform with a rough white surface (diameter, 6cm) was placed in the middle of the 1st quadrant (target quadrant) and immersed 1cm below the water surface. Four different black signs were settled in the middle side of each quadrant as spatial reference cues. On the 1st to 7th days (place navigation), each mouse was given four trials per day (60 seconds per trial) with a 10-minute rest time between trials. During the acquisition phase, the platform was fixed in the same location. Mice were released into the water from four directions in a random order each day. When a mouse succeeded in arriving on the platform within 60 seconds, it was permitted to remain on the platform for 10 seconds. If a mouse failed to reach the platform in 60 seconds, it would be guided onto the platform and allowed to remain there for 10 seconds. Latency to arrive onto the platform (latency to platform) and search strategy were recorded. On the 8th day, a probe trial was given at 24 hours after the last acquisition day. To perform the probe trial, the platform was removed from the water and the mice were allowed to swim for 60 seconds to search for the platform. The time spent crossing the platform site and the time spent in the target quadrant were recorded by MWM system software.

Open field maze (OFM)

Open field mazes are commonly used to evaluate spontaneous locomotor activity and exploratory behavior. In the present study, an open field test was performed as previously described [54]. Briefly, the open field system (Zhenghua Biological Instruments, China) includes four white Plexiglas (50×50×50 cm) open-field arenas, video acquisition, and an analysis system. During the test, mice were placed at one side of the arena and recorded for five minutes. Total traveled distance (mm), total time spent in the central zone, and resting time in the opening field were recorded.

Elevated plus maze (EPM)

The elevated plus maze (EPM) was performed to assess anxiety and activity among the mice according to a previously published method [55]. Briefly, the EPM system consists of two open arms and two enclosed arms with an open roof. The maze was elevated 40cm from the floor. During the experiment, mice were placed at extremity facing the walls of the enclosed arm and were allowed to explore the maze freely for five minutes. Total traveled distance, central entry frequency, and rest time in the maze were recorded using a video analysis system (Zhenghua Biological Instruments, China).

Tail suspension test (TST)

A tail suspension test (TST) was evaluated for depression behavior as previously described [56]. Briefly, mice were suspended in an inescapable but moderately stressful situation. They were suspended 40cm above the floor using a nylon string taped to the tip of their tails. By using a video analysis system (Zhenghua Biological Instruments, China), the rest time during a six-minute period was recorded. A lack of escape-related behavior was considered as immobility and depression.

MRI

An MRI was performed according to a previously reported process [57, 58]. Briefly, 12-month-old mice

received MRI scans on a 7.0-T BioSpec 70/20 MRI scanner (Bruker BioSpin, Germany) in a Shanghai cancer institute (Shanghai, China). For MRI handling procedures, all mice were anesthetized with 1.5% isoflurane (R510-22, RWD Life Science Co., China) with a mixture of 70% nitrogen and 30% oxygen. Respiration and body temperature were monitored during MRI scanning. T2-weighted images (T2WI): Three orthogonal multi-slice turbo rapid-acquisition with relaxation enhancement (RARE) were acquired to render slice-positioning uniform (slice thickness: 0.7mm; repetition time: 2500ms; echo time: 35ms; imaging frequency: 300.3206893ms; imaged nucleus: 1H; matrix: 256x256). All T2WI images were reconstructed by Paravision 6.0.1 and analyzed in Image J software to measure the thickness of the cortex. Diffusion images (DTI) were acquired using a "Bruker: DtiEpi SpinEcho" sequence (TE=0.68267ms, and TR=2800ms). The diffusion time was 12ms. The diffusion encoding duration was 5ms. A DTI diffusion scheme was used, and a total of 30 diffusion sampling directions were acquired. The b-value was 2040.17s/mm^2. The in-plane resolution was 0.140625mm. The slice thickness was 0.8mm. The diffusion tensor was calculated. By using DSI studio software, we measured the ROIs in the corpus callosum (CC) and external capsule (EC) regions to obtain fractional anisotropy (FA), axial diffusivity (Da), mean diffusivity (MD), and radial diffusivity (Dr) values.

Immunohistochemistry (IHC) staining

IHC staining was performed according to a previously reported process in our laboratory [15]. Briefly, mice were transcardially perfused with phosphate buffer saline (PBS) followed by 4% paraformaldehyde (PFA). The brains were post-fixed in 4% PFA for 24 hours and dehydrated in 30% sucrose for 72 hours. Then, the brains were cut into coronal sections (25μm thickness) in a cryostat and stored in Cryoprotectant. The brain sections were washed with PBS and 0.3% PBST (0.3% Triton X-100 in PBS) and then blocked with 5% goat serum in 0.3% PBST for 2 hours at room temperature. Brain sections were then incubated with primary antibodies for Aβ (anti-beta amyloid, 60342-1-Ig, Proteintech), GFAP (anti-GFAP, ab7260, Abcam), and NeuN (anti-NeuN, ab104224, Abcam) overnight at 4°C. After washing with 0.3% PBST, the sections were incubated with Alexa Flour® 488 secondary antibody for two hours at room temperature.

Western blot

Western blot was performed according to a previously reported process [34]. Briefly, the brain samples from four groups (n=6/per group) were collected, and then the proteins were extracted. A sodium dodecyl sulfate polyacrylamide gel (SDS-PAGE) electrophoresis system was used to separate the proteins, which were transferred onto 0.45-μm PVDF membranes (Millipore IPVH00010, MA, USA). The PVDF membranes were incubated with primary antibodies at 4°C overnight. After washing with washing buffer, the PVDF membranes were incubated with peroxidase-conjugated secondary antibodies. Signals were detected with a High-sig ECL Western Blotting Substrate (Tanon, Shanghai, China) and scanned with Bio-Rad ChemiDoc™ imaging systems. The primary antibodies used in this study were anti-Aβ (60342-1-Ig, Proteintech), anti-GFAP (ab7260, Abcam), anti-PSD95 (20665-1-AP, Proteintech), anti-Syn (17785-1-AP, Proteintech), anti-p-NFκB (#3033, Cell Signaling Technology), NFκB (#8242, Cell Signaling Technology), MyD88 (SAB3500472, Sigma-Aldrich), biglycan (ab58562, Abcam), HMGB1 (NB100-2322, Novus Biologicals), and anti-actin (ab822387, Abcam).

Statistical analysis

Data are presented as mean ± SEM. Statistical analyses were performed using GraphPad Prism 7.0. Comparison between two experimental groups was analyzed by a two-tailed t-test. Differences among multiple time spots were based on one or two-way ANOVA followed by the Sidak post hoc correction. The significance level was set to 0.05.

CONFLICTS OF INTEREST

The authors declare that there are no conflicts of interests regarding the publication of this paper.

FUNDING

This work was supported by National Nature Scientific Foundation of China to FH (81571469 and 81271268), ZZ (81501095), and XY (81671269), and Jiangsu Nature Scientific Foundation to ZZ (BK20150219).

REFERENCES

1. Ravari A, Mirzaei T, Kennedy D, Kazemi Arababadi M. Chronoinflammaging in Alzheimer; A systematic review on the roles of toll like receptor 2. Life Sci. 2017; 171:16–20. https://doi.org/10.1016/j.lfs.2017.01.003 PMID:28087373

2. Alzheimer's Association. 2018 Alzheimer's disease facts and figures. Alzheimers Dement. 2018; 14:367–429. https://doi.org/10.1016/j.jalz.2018.02.001

3. Scheltens P, Blennow K, Breteler MM, de Strooper B, Frisoni GB, Salloway S, Van der Flier WM. Alzheimer's disease. Lancet. 2016; 388:505–17.

https://doi.org/10.1016/S0140-6736(15)01124-1 PMID:26921134

4. Wang C, Najm R, Xu Q, Jeong DE, Walker D, Balestra ME, Yoon SY, Yuan H, Li G, Miller ZA, Miller BL, Malloy MJ, Huang Y. Gain of toxic apolipoprotein E4 effects in human iPSC-derived neurons is ameliorated by a small-molecule structure corrector. Nat Med. 2018; 24:647–57. https://doi.org/10.1038/s41591-018-0004-z PMID:29632371

5. Sanabria-Castro A, Alvarado-Echeverría I, Monge-Bonilla C. Molecular pathogenesis of Alzheimer's disease: an update. Ann Neurosci. 2017; 24:46–54. https://doi.org/10.1159/000464422 PMID:28588356

6. Guo Z, Zhang L, Wu Z, Chen Y, Wang F, Chen G. In vivo direct reprogramming of reactive glial cells into functional neurons after brain injury and in an Alzheimer's disease model. Cell Stem Cell. 2014; 14:188–202. https://doi.org/10.1016/j.stem.2013.12.001 PMID:24360883

7. Keren-Shaul H, Spinrad A, Weiner A, Matcovitch-Natan O, Dvir-Szternfeld R, Ulland TK, David E, Baruch K, Lara-Astaiso D, Toth B, Itzkovitz S, Colonna M, Schwartz M, et al. A unique microglia type associated with restricting development of Alzheimer's disease. Cell. 2017; 169:1276–1290.e1217. https://doi.org/10.1016/j.cell.2017.05.018 PMID:28602351

8. Santello M, Toni N, Volterra A. Astrocyte function from information processing to cognition and cognitive impairment. Nat Neurosci. 2019; 22:154–66. https://doi.org/10.1038/s41593-018-0325-8 PMID:30664773

9. Baizabal-Aguirre VM. Editorial: cross-talk mechanisms of wnt/beta-catenin signaling components with TLR-activated signaling molecules in the inflammatory response. Front Immunol. 2017; 8:1396. https://doi.org/10.3389/fimmu.2017.01396 PMID:29163478

10. Dorey E, Chang N, Liu QY, Yang Z, Zhang W. Apolipoprotein E, amyloid-beta, and neuroinflammation in Alzheimer's disease. Neurosci Bull. 2014; 30:317–30. https://doi.org/10.1007/s12264-013-1422-z PMID:24652457

11. Liu CC, Liu CC, Kanekiyo T, Xu H, Bu G. Apolipoprotein E and Alzheimer disease: risk, mechanisms and therapy. Nat Rev Neurol. 2013; 9:106–18. https://doi.org/10.1038/nrneurol.2012.263 PMID:23296339

12. Araque Caballero MA, Suárez-Calvet M, Duering M, Franzmeier N, Benzinger T, Fagan AM, Bateman RJ, Jack CR, Levin J, Dichgans M, Jucker M, Karch C, Masters CL, et al. White matter diffusion alterations precede symptom onset in autosomal dominant Alzheimer's disease. Brain. 2018; 141:3065–80. https://doi.org/10.1093/brain/awy229 PMID:30239611

13. Whitney NP, Eidem TM, Peng H, Huang Y, Zheng JC. Inflammation mediates varying effects in neurogenesis: relevance to the pathogenesis of brain injury and neurodegenerative disorders. J Neurochem. 2009; 108:1343–59. https://doi.org/10.1111/j.1471-4159.2009.05886.x PMID:19154336

14. Ye X, Kong D, Wang J, Ishrat T, Shi H, Ding X, Cui G, Hua F. MyD88 contributes to neuroinflammatory responses induced by cerebral ischemia/reperfusion in mice. Biochem Biophys Res Commun. 2016; 480:69–74. https://doi.org/10.1016/j.bbrc.2016.10.007 PMID:27717824

15. Hua F, Wang J, Ishrat T, Wei W, Atif F, Sayeed I, Stein DG. Genomic profile of Toll-like receptor pathways in traumatically brain-injured mice: effect of exogenous progesterone. J Neuroinflammation. 2011; 8:42. https://doi.org/10.1186/1742-2094-8-42 PMID:21549006

16. Lafon M, Megret F, Lafage M, Prehaud C. The innate immune facet of brain: human neurons express TLR-3 and sense viral dsRNA. J Mol Neurosci. 2006; 29:185–94. https://doi.org/10.1385/JMN:29:3:185 PMID:17085778

17. Too LK, McGregor IS, Baxter AG, Hunt NH. Altered behaviour and cognitive function following combined deletion of Toll-like receptors 2 and 4 in mice. Behav Brain Res. 2016; 303:1–8. https://doi.org/10.1016/j.bbr.2016.01.024 PMID:26774978

18. Chen L, Hu L, Zhao J, Hong H, Feng F, Qu W, Liu W. Chotosan improves Aβ1-42-induced cognitive impairment and neuroinflammatory and apoptotic responses through the inhibition of TLR-4/NF-κB signaling in mice. J Ethnopharmacol. 2016; 191: 398–407. https://doi.org/10.1016/j.jep.2016.03.038 PMID:26994819

19. Madar R, Rotter A, Waldman Ben-Asher H, Mughal MR, Arumugam TV, Wood WH 3rd, Becker KG, Mattson MP, Okun E. Postnatal TLR2 activation impairs learning and memory in adulthood. Brain Behav Immun. 2015; 48:301–12. https://doi.org/10.1016/j.bbi.2015.04.020 PMID:26021559

20. Park SJ, Lee JY, Kim SJ, Choi SY, Yune TY, Ryu JH. Toll-like receptor-2 deficiency induces schizophrenia-like behaviors in mice. Sci Rep. 2015; 5:8502. https://doi.org/10.1038/srep08502 PMID:25687169

21. Jin JJ, Kim HD, Maxwell JA, Li L, Fukuchi K. Toll-like receptor 4-dependent upregulation of cytokines in a transgenic mouse model of Alzheimer's disease. J Neuroinflammation. 2008; 5:23. https://doi.org/10.1186/1742-2094-5-23 PMID:18510752

22. Yousefi N, Sotoodehnejadnematalahi F, Heshmati-Fakhr N, Sayyah M, Hoseini M, Ghassemi S, Aliakbari S, and Pourbadie HG. Prestimulation of microglia through TLR4 pathway promotes interferon beta expression in a rat model of Alzheimer's disease. J Mol Neurosci. 2019; 67:495–503. https://doi.org/10.1007/s12031-018-1249-1 PMID:30610591

23. Chen K, Iribarren P, Hu J, Chen J, Gong W, Cho EH, Lockett S, Dunlop NM, Wang JM. Activation of Toll-like receptor 2 on microglia promotes cell uptake of Alzheimer disease-associated amyloid beta peptide. J Biol Chem. 2006; 281:3651–59. https://doi.org/10.1074/jbc.M508125200 PMID:16339765

24. Liu S, Liu Y, Hao W, Wolf L, Kiliaan AJ, Penke B, Rübe CE, Walter J, Heneka MT, Hartmann T, Menger MD, Fassbender K. TLR2 is a primary receptor for Alzheimer's amyloid β peptide to trigger neuroinflammatory activation. J Immunol. 2012; 188:1098–107. https://doi.org/10.4049/jimmunol.1101121 PMID:22198949

25. Richard KL, Filali M, Préfontaine P, Rivest S. Toll-like receptor 2 acts as a natural innate immune receptor to clear amyloid beta 1-42 and delay the cognitive decline in a mouse model of Alzheimer's disease. J Neurosci. 2008; 28:5784–93. https://doi.org/10.1523/JNEUROSCI.1146-08.2008 PMID:18509040

26. McDonald CL, Hennessy E, Rubio-Araiz A, Keogh B, McCormack W, McGuirk P, Reilly M, Lynch MA. Inhibiting TLR2 activation attenuates amyloid accumulation and glial activation in a mouse model of Alzheimer's disease. Brain Behav Immun. 2016; 58:191–200. https://doi.org/10.1016/j.bbi.2016.07.143 PMID:27422717

27. Suh EC, Jung YJ, Kim YA, Park EM, Lee SJ, Lee KE. Knockout of Toll-like receptor 2 attenuates Aβ25-35-induced neurotoxicity in organotypic hippocampal slice cultures. Neurochem Int. 2013; 63:818–25. https://doi.org/10.1016/j.neuint.2013.10.007 PMID:24161618

28. Rangasamy SB, Jana M, Roy A, Corbett GT, Kundu M, Chandra S, Mondal S, Dasarathi S, Mufson EJ, Mishra RK, Luan CH, Bennett DA, Pahan K. Selective disruption of TLR2-MyD88 interaction inhibits inflammation and attenuates Alzheimer's pathology. J Clin Invest. 2018; 128:4297–312. https://doi.org/10.1172/JCI96209 PMID:29990310

29. Schöll M, Lockhart SN, Schonhaut DR, O'Neil JP, Janabi M, Ossenkoppele R, Baker SL, Vogel JW, Faria J, Schwimmer HD, Rabinovici GD, Jagust WJ. PET Imaging of Tau deposition in the aging human brain. Neuron. 2016; 89:971–82. https://doi.org/10.1016/j.neuron.2016.01.028 PMID:26938442

30. Dansokho C, Heneka MT. Neuroinflammatory responses in Alzheimer's disease. J Neural Transm (Vienna). 2018; 125:771–79. https://doi.org/10.1007/s00702-017-1831-7 PMID:29273951

31. Lian H, Litvinchuk A, Chiang AC, Aithmitti N, Jankowsky JL, Zheng H. Astrocyte-microglia cross talk through complement activation modulates amyloid pathology in mouse models of Alzheimer's disease. J Neurosci. 2016; 36:577–89. https://doi.org/10.1523/JNEUROSCI.2117-15.2016 PMID:26758846

32. Kawai T, Akira S. The role of pattern-recognition receptors in innate immunity: update on Toll-like receptors. Nat Immunol. 2010; 11:373–84. https://doi.org/10.1038/ni.1863 PMID:20404851

33. Dong S, Zhang Q, Kong D, Zhou C, Zhou J, Han J, Zhou Y, Jin G, Hua X, Wang J, Hua F. Gender difference in the effect of progesterone on neonatal hypoxic/ischemic brain injury in mouse. Exp Neurol. 2018; 306:190–98. https://doi.org/10.1016/j.expneurol.2018.05.013 PMID:29772244

34. Hua F, Tang H, Wang J, Prunty MC, Hua X, Sayeed I, Stein DG. TAK-242, an antagonist for Toll-like receptor 4, protects against acute cerebral ischemia/reperfusion injury in mice. J Cereb Blood Flow Metab. 2015; 35:536–42. https://doi.org/10.1038/jcbfm.2014.240 PMID:25586141

35. Jones SV, Kounatidis I. Nuclear factor-kappa B and Azheimer disease, unifying genetic and environmental risk factors from cell to humans. Front Immunol. 2017; 8:1805. https://doi.org/10.3389/fimmu.2017.01805 PMID:29312321

36. Frank S, Copanaki E, Burbach GJ, Müller UC, Deller T. Differential regulation of toll-like receptor mRNAs in amyloid plaque-associated brain tissue of aged APP23

transgenic mice. Neurosci Lett. 2009; 453:41–44. https://doi.org/10.1016/j.neulet.2009.01.075 PMID:19429012

37. Zhang W, Wang LZ, Yu JT, Chi ZF, Tan L. Increased expressions of TLR2 and TLR4 on peripheral blood mononuclear cells from patients with Alzheimer's disease. J Neurol Sci. 2012; 315:67–71. https://doi.org/10.1016/j.jns.2011.11.032 PMID:22166855

38. Yu Y. and Ye RD. Microglial Aβ receptors in Alzheimer's disease. Cell Mol Neurobiol. 2015; 35:71-83. https://doi.org/10.1007/s10571-014-0101-6 PMID: 25149075

39. Pourbadie HG, Sayyah M, Khoshkholgh-Sima B, Choopani S, Nategh M, Motamedi F, Shokrgozar MA. Early minor stimulation of microglial TLR2 and TLR4 receptors attenuates Alzheimer's disease-related cognitive deficit in rats: behavioral, molecular, and electrophysiological evidence. Neurobiol Aging. 2018; 70:203–16. https://doi.org/10.1016/j.neurobiolaging.2018.06.020 PMID:30031930

40. Pascual M, Baliño P, Aragón CM, Guerri C. Cytokines and chemokines as biomarkers of ethanol-induced neuroinflammation and anxiety-related behavior: role of TLR4 and TLR2. Neuropharmacology. 2015; 89:352–59. https://doi.org/10.1016/j.neuropharm.2014.10.014 PMID:25446779

41. Jin S, Kim JG, Park JW, Koch M, Horvath TL, Lee BJ. Hypothalamic TLR2 triggers sickness behavior via a microglia-neuronal axis. Sci Rep. 2016; 6:29424. https://doi.org/10.1038/srep29424 PMID:27405276

42. Harsan LA, Poulet P, Guignard B, Steibel J, Parizel N, de Sousa PL, Boehm N, Grucker D, Ghandour MS. Brain dysmyelination and recovery assessment by noninvasive in vivo diffusion tensor magnetic resonance imaging. J Neurosci Res. 2006; 83:392–402. https://doi.org/10.1002/jnr.20742 PMID:16397901

43. Giannelli M, Cosottini M, Michelassi MC, Lazzarotti G, Belmonte G, Bartolozzi C, Lazzeri M. Dependence of brain DTI maps of fractional anisotropy and mean diffusivity on the number of diffusion weighting directions. J Appl Clin Med Phys. 2009; 11:176–190. https://doi.org/10.1120/jacmp.v11i1.2927 PMID:20160677

44. Tyszka JM, Readhead C, Bearer EL, Pautler RG, Jacobs RE. Statistical diffusion tensor histology reveals regional dysmyelination effects in the shiverer mouse mutant. Neuroimage. 2006; 29:1058–65. https://doi.org/10.1016/j.neuroimage.2005.08.037 PMID:16213163

45. Shen Z, Lei J, Li X, Wang Z, Bao X, Wang R. Multifaceted assessment of the APP/PS1 mouse model for Alzheimer's disease: applying MRS, DTI, and ASL. Brain Res. 2018; 1698:114–20. https://doi.org/10.1016/j.brainres.2018.08.001 PMID:30077647

46. Pekny M, Wilhelmsson U, Pekna M. The dual role of astrocyte activation and reactive gliosis. Neurosci Lett. 2014; 565:30–38. https://doi.org/10.1016/j.neulet.2013.12.071 PMID:24406153

47. Sadick JS, Liddelow SA. Don't forget astrocytes when targeting Alzheimer's disease. Br J Pharmacol. 2019; 176:3585–98. https://doi.org/10.1111/bph.14568 PMID:30636042

48. Gylys KH, Fein JA, Yang F, Wiley DJ, Miller CA, Cole GM. Synaptic changes in Alzheimer's disease: increased amyloid-beta and gliosis in surviving terminals is accompanied by decreased PSD-95 fluorescence. Am J Pathol. 2004; 165:1809–17. https://doi.org/10.1016/S0002-9440(10)63436-0 PMID:15509549

49. Sultana R, Banks WA, Butterfield DA. Decreased levels of PSD95 and two associated proteins and increased levels of BCl2 and caspase 3 in hippocampus from subjects with amnestic mild cognitive impairment: insights into their potential roles for loss of synapses and memory, accumulation of Abeta, and neurodegeneration in a prodromal stage of Alzheimer's disease. J Neurosci Res. 2010; 88:469–77. https://doi.org/10.1002/jnr.22227 PMID:19774677

50. Akwa Y, Gondard E, Mann A, Capetillo-Zarate E, Alberdi E, Matute C, Marty S, Vaccari T, Lozano AM, Baulieu EE, Tampellini D. Synaptic activity protects against AD and FTD-like pathology via autophagic-lysosomal degradation. Mol Psychiatry. 2018; 23:1530–40. https://doi.org/10.1038/mp.2017.142 PMID:28696431

51. Moreth K, Frey H, Hubo M, Zeng-Brouwers J, Nastase MV, Hsieh LT, Haceni R, Pfeilschifter J, Iozzo RV, Schaefer L. Biglycan-triggered TLR-2- and TLR-4-signaling exacerbates the pathophysiology of ischemic acute kidney injury. Matrix Biol. 2014; 35:143–51. https://doi.org/10.1016/j.matbio.2014.01.010 PMID:24480070

52. Roedig H, Nastase MV, Frey H, Moreth K, Zeng-Brouwers J, Poluzzi C, Hsieh LT, Brandts C, Fulda S, Wygrecka M, Schaefer L. Biglycan is a new high-affinity ligand for CD14 in macrophages. Matrix Biol.

2019; 77:4–22.
https://doi.org/10.1016/j.matbio.2018.05.006
PMID:29777767

53. Aucott H, Sowinska A, Harris HE, Lundback P. Ligation of free HMGB1 to TLR2 in the absence of ligand is negatively regulated by the C-terminal tail domain. Mol Med. 2018; 24:19.
https://doi.org/10.1186/s10020-018-0021-x
PMID:30134807

54. Seibenhener ML, Wooten MC. Use of the Open Field Maze to measure locomotor and anxiety-like behavior in mice. J Vis Exp. 2015; 96:e52434.
https://doi.org/10.3791/52434 PMID:25742564

55. Christakis DA, Ramirez JS, Ramirez JM. Overstimulation of newborn mice leads to behavioral differences and deficits in cognitive performance. Sci Rep. 2012; 2:546.
https://doi.org/10.1038/srep00546 PMID:22855702

56. Ip CW, Isaias IU, Kusche-Tekin BB, Klein D, Groh J, O'Leary A, Knorr S, Higuchi T, Koprich JB, Brotchie JM, Toyka KV, Reif A, Volkmann J. Tor1a+/- mice develop dystonia-like movements via a striatal dopaminergic dysregulation triggered by peripheral nerve injury. Acta Neuropathol Commun. 2016; 4:108.
https://doi.org/10.1186/s40478-016-0375-7
PMID:27716431

57. Montoliu-Gaya L, Güell-Bosch J, Esquerda-Canals G, Roda AR, Serra-Mir G, Lope-Piedrafita S, Sánchez-Quesada JL, Villegas S. Differential effects of apoE and apoJ mimetic peptides on the action of an anti-Aβ scFv in 3xTg-AD mice. Biochem Pharmacol. 2018; 155:380–92.
https://doi.org/10.1016/j.bcp.2018.07.012
PMID:30026023

58. Hattori Y, Enmi J, Kitamura A, Yamamoto Y, Saito S, Takahashi Y, Iguchi S, Tsuji M, Yamahara K, Nagatsuka K, Iida H, Ihara M. A novel mouse model of subcortical infarcts with dementia. J Neurosci. 2015; 35:3915–28.
https://doi.org/10.1523/JNEUROSCI.3970-14.2015
PMID:25740520